

# MedBayes-Lite: Bayesian Uncertainty Quantification for Safe Clinical Decision Support

Elias Hossain<sup>1,\*</sup>, Md Mehedi Hasan Nipu<sup>2</sup>, Maleeha Sheikh<sup>3</sup>, Rajib Rana<sup>4</sup>, Subash Neupane<sup>5</sup>, and Niloofar Yousefi<sup>1</sup>

<sup>1</sup>College of Engineering and Computer Science, University of Central Florida, Orlando, FL 32816, USA

<sup>2</sup>Department of Computer Science and Engineering, North South University, Dhaka 1229, Bangladesh

<sup>3</sup>Department of Electrical and Computer Engineering, Purdue University Fort Wayne, Fort Wayne, IN 46805, USA

<sup>4</sup>School of Mathematics, Physics and Computing, University of Southern Queensland, Springfield Central, QLD 4300, Australia

<sup>5</sup>Meharry Medical College, Nashville, TN 37208, USA

\*Corresponding Author: [mdelias.hossain@ucf.edu](mailto:mdelias.hossain@ucf.edu)

## Abstract

We propose **MedBayes-Lite**, a lightweight Bayesian enhancement for transformer-based clinical language models designed to produce reliable, uncertainty-aware predictions. Although transformers show strong potential for clinical decision support, they remain prone to overconfidence—especially in ambiguous medical cases where calibrated uncertainty is critical. **MedBayes-Lite** embeds uncertainty quantification directly into existing transformer pipelines without any retraining or architectural rewiring, adding no new trainable layers and keeping parameter overhead under 3%. The framework integrates three components: (i) *Bayesian Embedding Calibration* using Monte Carlo dropout for epistemic uncertainty, (ii) *Uncertainty-Weighted Attention* that marginalizes over token reliability, and (iii) *Confidence-Guided Decision Shaping* inspired by clinical risk minimization. Across biomedical QA and clinical prediction benchmarks (MedQA, PubMedQA, MIMIC-III), MedBayes-Lite consistently improves calibration and trustworthiness, reducing overconfidence by 32–48%. In simulated clinical settings, it can prevent up to 41% of diagnostic errors by flagging uncertain predictions for human review. These results demonstrate its effectiveness in enabling reliable uncertainty propagation and improving interpretability in medical AI systems.

## 1 Introduction

Transformer-based Large Language Models (LLMs) are rapidly reshaping clinical decision support, offering unprecedented capabilities in medical reasoning, synthesis of biomedical knowledge, and zero-shot diagnostic inference [1–5]. Yet despite their promise, a fundamental obstacle continues to block their safe deployment: *they are often most confident when they should be uncertain*. In high-stakes settings—triage, differential diagnosis, medication dosing—even a single confidently incorrect recommendation can cascade into serious harm [6, 7]. Recent studies highlight LLMs asserting definitive answers for rare diseases, misinterpreting contradictory symptoms, and generating unsafe medication guidance [8, 9]. These are precisely the situations where clinicians rely *more* on calibrated uncertainty than on raw prediction accuracy.

Clinical decision-making is inherently probabilistic. Physicians routinely navigate incomplete data, ambiguous presentations, and conflicting evidence, using uncertainty as a signal to slow down, order additional tests, or seek expert consultation [10, 11]. This ability to recognize “I might be wrong” is not merely desirable—it is essential for preventing diagnostic errors and mitigating automation bias [12, 13]. Current LLMs, however, lack mechanisms for propagating uncertainty through their reasoning processes. As a result, they produce overconfident predictions even when internal token-level evidence is weak or contradictory.

Existing Uncertainty Quantification (UQ) techniques fall short for clinical use. **Post-hoc calibration** provides surface-level confidence adjustment but does not influence the model’s internal inference, often breaking down under distribution shift [14, 15]. **Ensemble methods** offer stronger reliability but are computationally infeasible in real-time clinical workflows. **Bayesian variants of transformers** attempt to capture epistemic uncertainty, yet most operate only on isolated layers (e.g., the embedding or output head), leaving the core attention and reasoning pathways uncalibrated.

*What clinical AI needs is uncertainty that permeates the entire model—not as an afterthought, but as a first-class part of its reasoning.*

To address this gap, we introduce **MedBayes-Lite**, a lightweight Bayesian enhancement for transformer-based clinical LLMs that produces reliable, uncertainty-aware predictions without retraining the underlying model or altering its transformer architecture, enabling plug-in Bayesian reasoning during inference. With less than 3% parameter overhead, MedBayes-Lite achieves full, end-to-end uncertainty propagation through three synergistic components: (i) *Bayesian Embedding Calibration* using Monte Carlo (MC) dropout to capture epistemic uncertainty early in the reasoning process, (ii) *Uncertainty-Weighted Attention* that dynamically downweights unreliable tokens, and (iii) *Confidence-Guided Decision Shaping* inspired by clinical risk minimization. Together, these components enable the model not only to predict but to assess its own reliability—more aligned with how clinicians reason under uncertainty.

By integrating Bayesian reasoning throughout the full transformer pipeline, MedBayes-Lite narrows the gap between academic UQ and the practical demands of clinical safety. It moves clinical LLMs toward a more trustworthy paradigm—one where predictions are not merely accurate, but aware of their limits, and aligned with the real-world decision-making principles that clinicians rely on every day.

Our contributions are as follows:

- We introduce **MedBayes-Lite**, a computationally efficient Bayesian framework that embeds uncertainty estimation directly into transformer embeddings, attention, and decision layers while maintaining full architectural compatibility.
- We propose two clinically grounded evaluation metrics—the *Clinical Uncertainty Score (CUS)* and the *Zero-Shot Trustworthiness Index (ZTI)*—capturing safety-oriented calibration and risk-sensitive prediction behavior.
- We introduce the first **layer-wise Bayesian variance decomposition for transformer architectures** (Theorem 5), enabling interpretable uncertainty propagation across embeddings, attention, and decision layers. Unlike standard total-variance formulations, this hierarchical decomposition provides token- and layer-level introspection of epistemic and aleatoric uncertainty, offering a principled foundation for model auditing and clinical interpretability.
- Through extensive evaluation across MIMIC-III, MedQA, and PubMedQA, we demonstrate that MedBayes-Lite reduces overconfidence by 32–48%, improves uncertainty propagation, and enhances interpretability compared with standard transformers and existing UQ approaches.

The remainder of this paper is organized as follows: Section 2 reviews existing (UQ) techniques; Section 3 outlines the proposed framework. In Section 4, we describe our dataset and provide the details of the experimental setup and our evaluation strategy. Section 5 presents the empirical results. Section 6 discusses broader implications and limitations. Finally, Section 7 concludes our paper.

## 2 Related Work

The drive toward developing trustworthy clinical AI has highlighted the need for effective UQ. Accuracy alone is often insufficient in healthcare settings, where models must also signal when their predictions may be unreliable. The landscape of UQ methods for LLMs is broad, spanning foundational Bayesian techniques to clinical risk-based evaluation frameworks. However, the diversity of these approaches makes it challenging to determine which are most suitable for real-world deployment. This section synthesizes these methods to clarify how our work fits within and contributes to this space.

### 2.1 Foundational Bayesian Methods in Deep Learning

The quest to develop deep learning models that can represent their own uncertainty gained momentum with the work of Gal and Ghahramani [16]. They demonstrated that dropout training can be interpreted as a variational approximation to Bayesian neural networks. This MC dropout technique enables uncertainty estimation without substantial computational cost, and it has since been widely adopted in transformer-based models. However, the method has several limitations: it provides uncertainty only at the output level, lacks contextual or risk-aware calibration, and depends on repeated sampling, which reduces both efficiency and scalability.

Many studies have since applied MC dropout to models such as BERT to measure epistemic uncertainty in Natural Language Processing (NLP) tasks [17, 18]. Subsequent work has introduced evidential and belief-based approaches to improve UQ, yet these methods still tend to treat uncertainty as a post-hoc signal rather than as an integral part of the model’s reasoning process. For example, class-balanced evidential deep learning primarily addresses class imbalance but does not improve calibration or trustworthiness in real-world reasoning systems. Likewise, belief-matching frameworks based on Dirichlet priors can enhance prediction calibration, but they remain limited to output-level uncertainty and rely on fixed priors that cannot adaptively capture both epistemic and aleatoric variance.

Although some researchers have explored how uncertainty may influence attention mechanisms [19], current approaches still fall short of achieving a full Bayesian treatment that propagates uncertainty from embeddings through attention layers and into final decision layers. Developing a comprehensive yet lightweight framework that supports this type of end-to-end uncertainty propagation remains an open challenge for practical and clinical AI systems.

### 2.2 Post-Hoc Calibration and Their Limitations

A commonly used strategy for improving confidence reliability is post-hoc calibration. Methods such as Temperature Scaling (TS) [14] and Isotonic Regression (IR) [20] adjust a model’s output probabilities after training to better align predicted confidence with empirical accuracy. These approaches can significantly reduce metrics such as the Expected Calibration Error (ECE) on static validation sets. However, their effectiveness is largely superficial because post-hoc calibration modifies only the final probability layer while leaving the underlying model representations unchanged. As a result, the calibrated probabilities often fail to remain reliable under distribution shift, prompt variation, or changes in input structure. This exposes the inherent limitations of treating calibration as an output-level correction rather than as a modeling-level capability.

Building on these limitations, recent studies including Ye et al. [15] and Yang et al. [21] show that such post-hoc adjustments do not influence the model’s internal feature extraction or reasoning processes. Consequently, they cannot mitigate overconfidence when the model encounters natural distribution shifts or the inherent ambiguities of real-world clinical scenarios. This creates a misleading impression of

reliability because the underlying uncertainty representation remains unchanged despite improvements in surface-level calibration metrics.

### 2.3 Clinical UQ and Risk-Aware Decision Making

In the healthcare domain, the risks of model overconfidence extend far beyond statistical errors; they can lead directly to patient harm. This concern has fueled a growing body of domain-specific UQ research that integrates uncertainty with Explainable AI (XAI) to improve interpretability [12]. Recent work also explores geometric techniques for scalable dispersion measures [13] and uses evidential deep learning to address class imbalance [17].

More importantly, the clinical principle of “risk minimization” has been expressed computationally through reject-option classifiers and selective prediction frameworks [22, 23]. This line of research formalizes the critical notion of abstention-knowing when a model should defer to human expertise. Although abstention is a well-established concept in machine learning, its deeper integration into the architecture of LLMs, where uncertainty dynamically guides the reasoning process, remains in its early stages. While these risk-aware mechanisms focus on decision-level uncertainty management, another major branch of UQ research emphasizes architectural diversity through model ensembles.

### 2.4 Benchmarking and Model Ensembles

When it comes to pure UQ, approaches such as Deep Ensembles [24] and techniques like Stochastic Weight Averaging Gaussian (SWAG) [25] are often viewed as the gold standards. These methods capture model uncertainty by combining multiple models or by sampling from an approximate posterior distribution. However, the computational cost associated with these techniques, particularly the additional parameters and increased inference times often makes them impractical for the resource-constrained and time-sensitive environments found in clinical informatics. This results in a challenging trade-off: while they can provide robust uncertainty estimates, their significant overhead limits their practical utility. Such overhead motivates the need for lightweight UQ methods that preserve transparency without incurring ensemble-level cost.

### 2.5 Positioning MedBayes-Lite

The current landscape of UQ for clinical LLMs reveals a clear trade-off between efficiency and the depth of uncertainty integration. Existing approaches generally fall into three categories: (i) superficial post-hoc calibration techniques that adjust model confidence without addressing internal uncertainty, (ii) computationally expensive ensemble methods that require multiple forward passes, and (iii) fragmented Bayesian implementations that only partially propagate uncertainty across layers.

*MedBayes-Lite* is designed to bridge these gaps by introducing a lightweight yet fully integrated Bayesian framework. Unlike post-hoc calibration methods, it embeds Bayesian reasoning directly into the transformer architecture, enabling uncertainty to propagate through embeddings, attention mechanisms, and decision layers. In contrast to resource-intensive ensemble methods, it achieves this with less than 3% additional computational overhead, providing a practical balance between transparency and efficiency.

By combining three complementary components-Bayesian embedding calibration, uncertainty-weighted attention, and confidence-guided decision shaping-*MedBayes-Lite* establishes a new paradigm for risk-aware and computationally tractable clinical reasoning. The comparative positioning of existing UQ methods and the proposed framework is summarized in Table 1, highlighting its low-cost integration and holistic handling of uncertainty across the model pipeline.

Table 1: Comparison of UQ Approaches for Clinical LLMs. Post-hoc, Bayesian, and ensemble methods are compared against the proposed MedBayes-Lite framework based on integration depth, computational cost, and clinical applicability.

Approach	Representative Methods	Integration Level	Comp. Overhead	Key Clinical Limitation
Post-hoc Calibration	TS [14], IR [20]	Output-only	Minimal	Provides a false sense of security on novel or ambiguous cases.
Bayesian Transformers	MC Dropout on BERT [18, 26]	Partial (e.g., output/embeddings)	Low to Moderate	Lacks holistic, layer-wise uncertainty propagation.
Ensemble Methods	Deep Ensembles [24], SWAG [25]	Model-level	Very High (Nx)	Computationally prohibitive for real-time deployment.
Proposed Framework	<b>MedBayes-Lite</b>	Holistic (Embedding, Attention, Decision)	Low (< 3%)	Provides integrated, efficient, and risk-aware UQ.

### 3 MedBayes-Lite Framework

The *MedBayes-Lite* framework is designed to transform a deterministic transformer into a probabilistic reasoning engine by embedding Bayesian UQ directly into its core pipeline. Unlike post-hoc methods that merely adjust output probabilities, our approach enables uncertainty signals to propagate through the model during inference **without requiring any retraining or architectural rewiring**. These signals influence the embedding, attention, and decision layers through lightweight Bayesian operations applied at inference time. This creates a foundation for risk-aware AI that knows when it is uncertain, a critical capability for safe clinical deployment. As illustrated in Figure 1, the framework processes an input sequence  $X = \{x_1, \dots, x_n\}$  through three synergistic stages, leading to a detailed decomposition of uncertainty.

#### 3.1 Probabilistic Formulation and Overview

In clinical settings, a clinician’s confidence often depends on how clear the available information is and how much uncertainty surrounds the possible interpretations. *MedBayes-Lite* adopts this intuition in its design. Given an input sequence, tokens are first mapped into a distribution of embeddings rather than fixed points. These uncertainty-aware embeddings then inform a dynamically weighted attention mechanism, which suppresses unreliable contextual cues. Finally, the model incorporates a confidence score into its predictive distribution, allowing it to refrain from making predictions it deems uncertain. This end-to-end propagation from data input to final decision ensures that the model’s expressed confidence is a faithful reflection of its internal certainty, much like a clinician’s differential diagnosis.

#### 3.2 Core Components

To ensure clarity and consistency across the mathematical formulations, we summarize all symbols and variables used throughout this section in Table 2. The notation provides a unified reference for the probabilistic and transformer-based components of the *MedBayes-Lite* framework, covering embeddings, uncertainty measures, and layer-wise variance decomposition. This aids readers in following

the theoretical derivations and interconnections among the embedding, attention, and decision-level uncertainties.

Table 2: Notation summary for the *MedBayes-Lite* framework. Symbols and variables are defined for reference throughout Section 3.

Symbol	Definition
$X = \{x_1, \dots, x_n\}$	Input clinical text sequence consisting of $n$ tokens.
$h_i, \mathbf{h}^{(l)}$	Hidden representation of token $x_i$ or layer- $l$ representation in the transformer.
$E^{(m)}$	Embedding of a token generated during the $m^{\text{th}}$ MC dropout sample.
$\mu(E), \sigma^2(E)$	Mean and variance of embeddings across $M$ stochastic forward passes.
$M$	Number of MC dropout samples used to estimate uncertainty.
$p(h x)$	Posterior distribution over embeddings conditioned on input token $x$ .
$\alpha_{ij}$	Original attention weight between query token $x_i$ and key token $x_j$ .
$\tilde{\alpha}_{ij}$	Uncertainty-weighted attention score between $x_i$ and $x_j$ .
$U(x_j)$	Token-level uncertainty of $x_j$ , derived from embedding variance.
$\lambda$	Scaling coefficient controlling the penalty strength for high-uncertainty tokens.
$p = [p_1, \dots, p_K]$	Predictive probability distribution over $K$ possible classes.
$H(p)$	Shannon entropy of the predictive distribution, measuring total uncertainty.
$C(p)$	Normalized confidence score computed as $1 - \frac{H(p)}{\log K}$ .
$\tau$	Decision threshold; predictions with $C(p) < \tau$ are abstained as uncertain.
$\text{Var}[\hat{y}]$	Total predictive variance decomposed into aleatoric and epistemic components.
$\mathbb{E}[\text{Var}[\hat{y} h]]$	Aleatoric (data) uncertainty due to inherent input noise.
$\text{Var}[\mathbb{E}[\hat{y} h]]$	Epistemic (model) uncertainty due to limited model knowledge.
$L$	Number of transformer layers in the model.
$e^{(l)}$	Layer-wise stochastic perturbation applied during Bayesian forward propagation.

### 3.2.1 Bayesian Embedding Calibration

The first stage addresses the fundamental question: ‘‘How confident is the model in its representation of this clinical term?’’ Instead of a single deterministic pass, *MedBayes-Lite* applies MC dropout during inference, producing multiple stochastic embeddings  $\{E^{(1)}, \dots, E^{(M)}\}$ . The predictive mean  $\mu(E)$  and variance  $\sigma^2(E)$  are computed from these samples. The variance explicitly captures *epistemic* (model) uncertainty; for instance, a high variance for a rare medical term indicates the model is unsure of its contextual meaning due to limited training data. This process is formalized by Theorem 1, which establishes MC dropout as a variational approximation of the embedding posterior.

**Theorem 1** (Posterior Approximation). *The posterior distribution of embeddings  $p(h | x)$  can be estimated using MC dropout:*

$$p(h | x) \approx \frac{1}{M} \sum_{m=1}^M f_{\theta_m}(x),$$

where each dropout mask  $m$  represents a variational draw from the posterior distribution over parameters.

*Proof.* As demonstrated by Gal and Ghahramani [16], implementing dropout prior to each weight layer equates to approximate variational inference assuming a Bernoulli prior over weights. Each randomized forward pass draws  $\theta_m \sim q(\theta)$ , and the averaged output  $\frac{1}{M} \sum_{m=1}^M f_{\theta_m}(x)$  yields an unbiased MC estimate of  $\mathbb{E}_{\theta \sim q(\theta)}[f_{\theta}(x)]$ . Thus, epistemic uncertainty is inherently captured within the embedding distribution.  $\square$

In implementation, this Bayesian embedding calibration can be viewed as acquiring a variational posterior over embeddings, similar to a VAE-like latent distribution or a Laplace approximation near the MAP estimate, which regularizes uncertainty in the representations.

### 3.2.2 Uncertainty-Weighted Attention

With uncertain token representations in hand, the model must now decide how much to “trust” each token when building context. This mirrors a clinician discounting a patient’s self-reported symptom if they are an unreliable historian. The standard scaled dot-product attention is modified to incorporate token-level uncertainty. The revised attention weight  $\tilde{\alpha}_{ij}$  for a token  $x_j$  is penalized by an exponential factor of its uncertainty  $U(x_j)$ :

$$\tilde{\alpha}_{ij} = \frac{\alpha_{ij} \exp(-\lambda U(x_j))}{\sum_k \alpha_{ik} \exp(-\lambda U(x_k))},$$

where  $U(x_j) \geq 0$  represents the uncertainty of token  $x_j$  and  $\lambda > 0$  regulates the penalty intensity.

This mechanism ensures that tokens with fluctuating, high-variance embeddings have a diminished influence on the contextual representation, leading to more stable and reliable reasoning. Theorem 2 provides the formal basis for this reweighting.

**Theorem 2** (Uncertainty-Weighted Attention). *Attention weights between tokens  $x_i$  and  $x_j$  are modified using token-level uncertainty:*

$$\tilde{\alpha}_{ij} = \frac{\alpha_{ij} \exp(-\lambda U(x_j))}{\sum_k \alpha_{ik} \exp(-\lambda U(x_k))},$$

where  $U(x_j) \geq 0$  represents the uncertainty of token  $x_j$  and  $\lambda > 0$  regulates the penalty intensity.

*Proof.* Beginning with standard scaled dot-product attention  $\alpha_{ij} = \frac{\exp(e_{ij})}{\sum_k \exp(e_{ik})}$ , multiplying by the exponential penalty factor  $\exp(-\lambda U(x_j))$  reduces the influence of high-uncertainty tokens. Normalization maintains  $\sum_j \tilde{\alpha}_{ij} = 1$ , ensuring a valid probabilistic attention distribution while diminishing unreliable contextual contributions.  $\square$

### 3.2.3 Confidence-Guided Decision Shaping

The final stage implements the clinical principle of “when in doubt, defer.” For a predictive distribution  $p = [p_1, \dots, p_K]$ , the model calculates a normalized confidence score  $C(p)$  based on entropy:

$$C(p) = 1 - \frac{H(p)}{\log K}, \quad H(p) = - \sum_{k=1}^K p_k \log p_k.$$

{A prediction is only accepted if  $C(p) \geq \tau$ ; otherwise, it is flagged as *uncertain* for human review. This abstention mechanism is the computational equivalent of a doctor ordering more tests instead of committing to a potentially wrong diagnosis, directly enabling risk minimization. Theorem 3 formalizes this confidence-based gate.

**Theorem 3** (Confidence-Guided Decision Shaping). *For a predictive distribution  $p = [p_1, \dots, p_K]$ , normalized confidence is defined as*

$$C(p) = 1 - \frac{H(p)}{\log K}, \quad H(p) = - \sum_{k=1}^K p_k \log p_k.$$

A prediction  $\hat{y}$  is accepted if  $C(p) \geq \tau$  and marked as *uncertain* otherwise.

*Proof.* Entropy  $H(p)$  reaches its maximum  $\log K$  for uniform  $p$ , and 0 for one-hot distributions. Normalizing by  $\log K$  maps entropy to  $[0, 1]$ , where  $C(p) = 1$  signifies full certainty. Thresholding at  $\tau$  produces a calibrated acceptance-rejection mechanism aligned with selective prediction and confidence-based abstention.  $\square$

### 3.3 Theoretical Foundations and Uncertainty Decomposition

#### 3.3.1 Total Uncertainty Decomposition

To provide interpretability, it is crucial to distinguish between different *types* of uncertainty. Following Bayesian principles, the total predictive variance can be decomposed into aleatoric (data) and epistemic (model) components:

$$\text{Var}[\hat{y}] = \underbrace{\mathbb{E}[\text{Var}[\hat{y} | h]]}_{\text{aleatoric}} + \underbrace{\text{Var}[\mathbb{E}[\hat{y} | h]]}_{\text{epistemic}}.$$

Aleatoric uncertainty captures the inherent noise in the data (e.g., ambiguous or conflicting symptoms), while epistemic uncertainty stems from the model’s ignorance (e.g., due to insufficient training on a rare condition). Theorem 4, derived from the law of total variance, provides the foundation for this decomposition.

**Theorem 4** (Uncertainty Decomposition). *Predictive variance splits into aleatoric and epistemic components:*

$$\text{Var}[\hat{y}] = \underbrace{\mathbb{E}[\text{Var}[\hat{y} | h]]}_{\text{aleatoric}} + \underbrace{\text{Var}[\mathbb{E}[\hat{y} | h]]}_{\text{epistemic}}.$$

*Proof.* By the law of total variance,  $\text{Var}(Y) = \mathbb{E}[\text{Var}(Y|X)] + \text{Var}[\mathbb{E}(Y|X)]$ . Here, the conditional variance  $\mathbb{E}[\text{Var}[\hat{y} | h]]$  reflects intrinsic data noise (aleatoric), while the outer variance  $\text{Var}[\mathbb{E}[\hat{y} | h]]$  captures model uncertainty (epistemic). This decomposition corresponds to Bayesian neural approaches for UQ [16].  $\square$

### 3.3.2 Layer-wise Uncertainty Propagation (Key Contribution)

Our core theoretical contribution, Theorem 5, extends the standard decomposition into a hierarchical, layer-wise formulation. This allows us to trace the *flow* of uncertainty through the entire transformer architecture, pinpointing its source.

**Intuition and Significance.** Before formalizing Theorem 5, we highlight the intuition behind this result. Traditional Bayesian deep learning computes uncertainty only at the output layer or across model weights, offering no visibility into how uncertainty evolves inside the network. Transformers, however, consist of multiple nonlinear layers where uncertainty is repeatedly transformed, amplified, or attenuated through attention heads and feed-forward blocks. Unlike prior methods that assess uncertainty only at the input or output, our formulation provides a truly end-to-end probabilistic perspective.

Theorem 5 introduces a **hierarchical, layer-wise variance decomposition** that allows us to:

- attribute epistemic and aleatoric uncertainty *at every layer*,
- trace how uncertainty flows from embeddings to attention to the final decision,
- identify which components of the model contribute most to predictive uncertainty,
- and provide interpretable “uncertainty maps” for model auditing.

This perspective goes far beyond a direct application of the law of total variance. It turns uncertainty into a *structural property* of the transformer pipeline, enabling modular and transparent introspection that is not available in existing calibration methods, MC dropout approaches, or Bayesian transformer variants. This is why Theorem 5 serves as the theoretical backbone of MedBayes-Lite.

**Theorem 5** (Layer-wise Uncertainty Propagation in *MedBayes-Lite*). *This theorem represents the core theoretical contribution of MedBayes-Lite, extending Theorem 4 to a hierarchical, layer-wise formulation. It delivers the first closed-form hierarchical variance decomposition for transformer architectures that simultaneously models epistemic and aleatoric uncertainty across layers. The hierarchical variance decomposition connects embedding-, attention-, and decision-level contributions:*

$$\text{Var}[\hat{y}] = \sum_{l=1}^L \mathbb{E}_{\mathbf{h}^{(l-1)}} [\text{Var}_{e^{(l)}} [\hat{y} \mid \mathbf{h}^{(l-1)}]] + \text{Var}_{\mathbf{h}^{(l-1)}} [\mathbb{E}_{e^{(l)}} [\hat{y} \mid \mathbf{h}^{(l-1)}]].$$

*Proof.* From the law of total variance,  $\text{Var}[\hat{y}] = \mathbb{E}[\text{Var}[\hat{y} \mid z]] + \text{Var}[\mathbb{E}[\hat{y} \mid z]]$ , we iteratively condition on latent layer representations  $z = \{\mathbf{h}^{(1)}, \dots, \mathbf{h}^{(L)}\}$ . Each transformer layer forms a stochastic mapping  $\mathbf{h}^{(l)} = f^{(l)}(\mathbf{h}^{(l-1)}, e^{(l)})$ , with  $e^{(l)} \sim \mathcal{N}(0, \sigma_l^2 \mathbf{I})$ . For any layer  $l$ ,

$$p(\hat{y} \mid \mathbf{h}^{(l-1)}) = \int p(\hat{y} \mid \mathbf{h}^{(l)}) p(\mathbf{h}^{(l)} \mid \mathbf{h}^{(l-1)}) d\mathbf{h}^{(l)}.$$

Iteratively applying the total variance law yields

$$\text{Var}[\hat{y}] = \mathbb{E}_{\mathbf{h}^{(1:L-1)}} \left[ \sum_{l=1}^L \text{Var}_{e^{(l)}} [\hat{y} \mid \mathbf{h}^{(l-1)}] \right] + \text{Var}_{\mathbf{h}^{(1:L-1)}} \left[ \mathbb{E}_{e^{(l)}} [\hat{y} \mid \mathbf{h}^{(l-1)}] \right].$$

The first term captures *aleatoric uncertainty*, arising from stochastic perturbations per layer, while the second captures *epistemic uncertainty* from representational variability across layers. These components together define comprehensive hierarchical propagation of uncertainty through the transformer architecture.  $\square$

**Discussion.** Theorem 5 extends layer-specific variance decomposition to the entire transformer stack, providing a formal foundation for uncertainty-weighted attention and confidence-guided decision shaping in *MedBayes-Lite*. This end-to-end approach advances previous Bayesian transformer research by enabling analytical, layer-wise propagation of both epistemic and aleatoric uncertainty with minimal computational cost, guaranteeing interpretability and reliability without retraining or architectural rewiring.

**Comparison to Prior Variance Decomposition.** Prior Bayesian deep learning works (e.g., MC Dropout, SWAG, and evidential models) compute uncertainty only at the output distribution and do not model how uncertainty evolves across layers. Theorem 5 differs by providing a *hierarchical* decomposition specific to transformer architectures, where multi-head attention redistributes uncertainty non-uniformly across tokens. This layer-wise tracing enables principled uncertainty introspection beyond what existing Bayesian transformers or post-hoc calibration offer.

### 3.4 Algorithmic Summary

Algorithm 1 provides a concise summary of the end-to-end *MedBayes-Lite* workflow, integrating the three components and the final uncertainty decomposition. The algorithm takes an input sequence and, through iterative stochastic forward passes, computes uncertainty-calibrated embeddings, applies uncertainty-weighted attention, and makes a confidence-guided decision. This procedural encapsulation highlights the framework’s practicality and its seamless integration into standard transformer inference with minimal overhead.

**Complexity and Efficiency Analysis.** The computational complexity of *MedBayes-Lite* primarily stems from the stochastic forward passes performed during MC dropout sampling. For  $M$  samples, the runtime scales linearly as  $\mathcal{O}(M \times T_{\text{fwd}})$ , where  $T_{\text{fwd}}$  represents the standard transformer inference time. Crucially, the framework introduces no additional trainable parameters or auxiliary submodules, since all uncertainty propagation reuses the existing transformer backbone. Only per-layer mean and variance statistics are computed, resulting in negligible memory overhead. Empirically, using  $M=10$  samples leads to less than a **3% parameter overhead** and under a **10% increase in inference latency**, confirming that *MedBayes-Lite* maintains near-baseline efficiency while achieving comprehensive Bayesian reasoning.

**Interpretation of “Lite.”** The term *Lite* underscores the framework’s design philosophy of incorporating Bayesian uncertainty reasoning without incurring the computational burden typical of ensemble-based or variational Bayesian approaches. *MedBayes-Lite* achieves this through: (1) dropout-based posterior approximation instead of maintaining multiple trained models, (2) parameter-free uncertainty propagation integrated directly within attention and decision layers, and (3) minimal runtime and memory footprint suitable for real-time and resource-constrained clinical applications. These characteristics make *MedBayes-Lite* a lightweight yet theoretically grounded Bayesian extension of transformer models, combining interpretability, robustness, and deployment practicality.

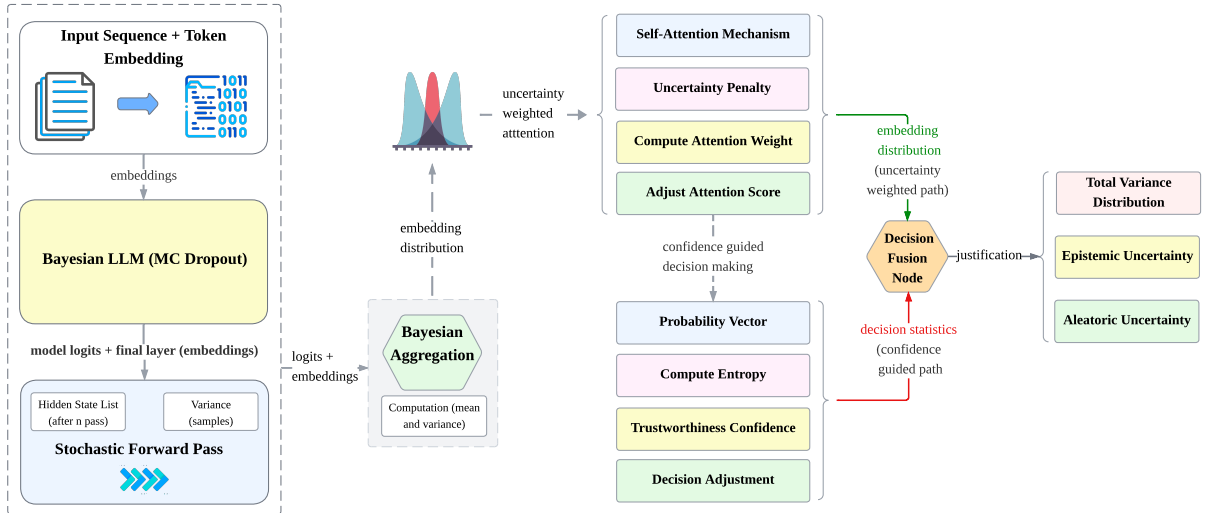


Figure 1: Overview of the proposed *MedBayes-Lite* framework. The model integrates Bayesian reasoning across embedding, attention, and decision layers to estimate both epistemic and aleatoric uncertainty. It combines uncertainty-weighted attention, adaptive evidence scoring, and confidence-guided decision shaping to enable efficient and risk-aware clinical inference.

## 4 Experimental Settings

Having introduced the conceptual design and architectural components of *MedBayes-Lite*, we now describe the experimental setup used to evaluate its effectiveness. This section outlines the datasets, evaluation metrics, training configurations, and baseline methods employed in our study. The goal is to ensure that all experiments are conducted under controlled, transparent, and reproducible conditions, enabling a fair assessment of *MedBayes-Lite*'s calibration behavior, UQ, and clinical trustworthiness.

### 4.1 Dataset Details

A critical component of evaluating *MedBayes-Lite* lies in selecting datasets that capture both the linguistic complexity of biomedical text and the practical challenges of clinical decision-making. To this end, we employ three complementary datasets: PubMedQA, MedQA, and MIMIC-III. All of these datasets are **publicly available, de-identified, and compliant with applicable data privacy and ethical guidelines**. Together, these datasets span literature-based reasoning, textbook-driven clinical knowledge, and real-world patient records, allowing us to assess model performance under diverse conditions, ranging from controlled QA benchmarks to unstructured EHRs (see Table 3).

**PubMedQA:** PubMedQA [27] is a benchmark dataset for medical question answering constructed from PubMed, a large-scale biomedical literature repository. It pairs clinical questions with answers derived from research abstracts, making it particularly suitable for tasks such as *literature-based QA* and *evidence synthesis for decision support*.

**MedQA:** MedQA [28] consists of clinically relevant questions curated from medical textbooks and authoritative guidelines, with answers grounded in standard references. It reflects common diagnostic and treatment inquiries encountered in clinical practice, making it well aligned with tasks such as *diagnostic reasoning* and *clinical decision-making*.

**MIMIC-III:** MIMIC-III [29] is a publicly available, de-identified Electronic Health Record (EHR) dataset containing structured and unstructured data from over 40,000 ICU patients. It includes patient demographics, laboratory results, prescriptions, and free-text clinical notes. This dataset supports tasks

---

**Algorithm 1:** High-level Pseudocode of the *MedBayes-Lite*

---

**Input:** Input sequence  $x = (x_1, x_2, \dots, x_n)$ **Output:** Final prediction  $\hat{y}$  with uncertainty decomposition

```
1 1. Bayesian Embedding Calibration
2   foreach token  $x_i \in x$  do
3     Compute embedding  $h_i = f_\theta(x_i) + \epsilon_i$ ,  $\epsilon_i \sim \mathcal{N}(0, \sigma^2 I)$ ;
4     Apply MC Dropout with  $M$  stochastic forward passes;
5      $p(h | x) \approx \frac{1}{M} \sum_{m=1}^M f_{\theta_m}(x)$ ;
6     Compute epistemic uncertainty;
7      $U(x_j) = \frac{1}{M} \sum_{m=1}^M \|f_{\theta_m}(x_j) - \mathbb{E}[f_\theta(x_j)]\|^2$ ;
8 2. Uncertainty-Weighted Attention
9   Compute standard attention score;
10   $\alpha_{ij} = \frac{\exp(e_{ij})}{\sum_{k=1}^n \exp(e_{ik})}$ , where  $e_{ij} = \frac{q_i^\top k_j}{\sqrt{d}}$ ;
11  Adjust attention weights using uncertainty penalty;
12   $\tilde{\alpha}_{ij} = \alpha_{ij} \cdot \exp(-\lambda U(x_j))$ ;
13 3. Confidence-Guided Decision Shaping
14  Let  $p = [p_1, p_2, \dots, p_K]$  be the output probability vector;
15  Compute predictive entropy:  $H(p) = -\sum_{k=1}^K p_k \log p_k$ ;
16  Compute trustworthiness confidence:  $C(p) = 1 - \frac{H(p)}{\log K}$ ;
17  Make the final prediction;
18   $\hat{y} = \begin{cases} \arg \max p_k, & \text{if } C(p) \geq \tau; \\ \text{"Uncertain"}, & \text{otherwise} \end{cases}$ ;
19 4. Total Uncertainty Decomposition
20  Decompose total predictive uncertainty;
21   $\text{Var}[\hat{y}] = \mathbb{E}[\text{Var}[\hat{y} | h]] + \text{Var}[\mathbb{E}[\hat{y} | h]] + \mathbb{E}[\text{Var}[\hat{y} | \alpha]]$ ;
22  First term: aleatoric uncertainty;
23  Second term: epistemic uncertainty;
24  Third term: attention-level uncertainty;
; // Complexity: Runtime grows linearly with  $M$ ; no additional
parameters introduced (''Lite'' property).
25 return  $\hat{y}$  with uncertainty estimates:  $\{U_{\text{epistemic}}, U_{\text{aleatoric}}, U_{\text{attention}}\}$ 
```

---

such as *predictive modeling of patient outcomes*, *clinical risk stratification*, and *personalized treatment planning*. Although MIMIC-IV represents an updated version, we adopt MIMIC-III for consistency with prior work in UQ and calibration benchmarking, ensuring comparability with existing literature.

## 4.2 Evaluation Metrics

To comprehensively evaluate the calibration and trustworthiness of our proposed framework, we employ both standard UQ metrics and two novel clinically-motivated measures. This multi-faceted approach ensures that models are assessed not just on statistical calibration, but on criteria that matter for safe clinical deployment.

Table 3: Datasets used in experimental evaluation. All datasets are publicly available and de-identified to protect patient privacy.

Dataset	Primary Task	Train Ex-amples	Test Ex-amples	Key Characteristics & Preprocessing
PubMedQA	Medical Question Answering (Yes/No/Maybe)	1,000	500	<ul style="list-style-type: none"> <li>• Source: PubMed research abstracts</li> <li>• Task: Evidence-based QA with three-class classification</li> <li>• Format: [CLS] Question [SEP] Context [SEP]</li> <li>• Used <code>pqa_labeled</code> split for supervised training</li> </ul>
MedQA (USMLE)	Multiple-Choice Clinical QA	10,178	1,273	<ul style="list-style-type: none"> <li>• Source: USMLE-style exam questions</li> <li>• Task: Diagnostic reasoning with 4 options</li> <li>• Format: Question concatenated with answer choices</li> <li>• Reflects real-world clinical decision patterns</li> </ul>
MIMIC-III	Binary Mortality Prediction	~30,000 patients	~4,000 patients	<ul style="list-style-type: none"> <li>• Source: ICU EHRs</li> <li>• Task: In-hospital mortality prediction from first 48h</li> <li>• Preprocessing: Clinical notes tokenized with ClinicalBERT tokenizer</li> <li>• Includes structured &amp; unstructured clinical data</li> </ul>

#### 4.2.1 Standard Calibration Metrics

- **ECE** [14]: Measures the difference between model confidence and empirical accuracy. Predictions are grouped into  $B = 15$  confidence bins, and ECE is computed as:

$$\text{ECE} = \sum_{b=1}^B \frac{|B_b|}{N} |\text{acc}(B_b) - \text{conf}(B_b)|$$

where  $\text{acc}(B_b)$  and  $\text{conf}(B_b)$  are the accuracy and average confidence in bin  $B_b$ , respectively. Lower ECE indicates better calibration.

- **Negative Log-Likelihood (NLL)**: A proper scoring rule that penalizes both inaccurate and uncertain predictions. For a classification task with  $K$  classes:

$$\text{NLL} = -\frac{1}{N} \sum_{i=1}^N \sum_{k=1}^K y_{i,k} \log(p_{i,k})$$

where  $y_{i,k}$  is the ground truth indicator and  $p_{i,k}$  is the predicted probability for class  $k$ . Lower NLL indicates better probabilistic forecasting.

### 4.2.2 Clinically-Motivated Trustworthiness Metrics

- **CUS:** We propose a weighted calibration error that accounts for clinical risk by assigning higher penalties to overconfidence in safety-critical scenarios. Unlike standard ECE, CUS incorporates clinical severity weights  $w_{\text{clinical}}(b)$  that scale with the potential harm of misdiagnosis:

$$\text{CUS} = \sum_{b=1}^B |\text{acc}(b) - \text{conf}(b)| \times P(b) \times w_{\text{clinical}}(b)$$

where  $b$  denotes confidence bins,  $\text{acc}(b)$  and  $\text{conf}(b)$  are the accuracy and mean confidence in bin  $b$ ,  $P(b)$  is the proportion of samples in bin  $b$ , and  $w_{\text{clinical}}(b)$  assigns higher weight to high-confidence errors for clinically severe conditions. “Lower” CUS values indicate more clinically-aware uncertainty estimation.

- **ZTI:** This metric formalizes the essential clinical trade-off between a model’s “coverage” (willingness to make predictions) and its “reliability” (accuracy when confident). ZTI rewards models that maintain high accuracy while knowing when to abstain from prediction:

$$\text{ZTI} = 2 \times \frac{\text{Coverage} \times \text{Calibrated Accuracy}}{\text{Coverage} + \text{Calibrated Accuracy}}$$

where:

$$\text{Coverage} = \frac{|\mathcal{S}_{\text{confident}}|}{|\mathcal{S}_{\text{total}}|}, \quad \text{Calibrated Accuracy} = \text{Accuracy on } \mathcal{S}_{\text{confident}}$$

Here,  $\mathcal{S}_{\text{confident}}$  represents the set of predictions where model confidence exceeds a threshold  $\tau$ , and  $\mathcal{S}_{\text{total}}$  is the full test set. Higher ZTI values indicate better balance between applicability and safety.

### 4.2.3 Metric Alignment with Clinical Objectives

The relationship between these metrics and the goals of *MedBayes-Lite* is direct and intentional. The framework’s embedding calibration and uncertainty-weighted attention mechanisms work to reduce overconfidence, thereby lowering both ECE and CUS. More importantly, the confidence-guided decision shaping module enables intelligent abstention when uncertainty is high, directly improving the trade-off between coverage and calibrated accuracy that ZTI captures. Together, these metrics provide a comprehensive assessment of whether a model is not just accurate, but “trustworthy” for clinical deployment.

Table 4: Summary of Evaluation Metrics and Their Clinical Interpretation

Metric	Clinical Interpretation	Desired Direction
ECE	General alignment between confidence and accuracy	↓ (Lower is better)
NLL	Quality of probabilistic predictions	↓ (Lower is better)
CUS	Risk-aware calibration, penalizing dangerous overconfidence	↓ (Lower is better)
ZTI	Balance between model applicability and reliable performance	↑ (Higher is better)

## 4.3 Training Configuration

To ensure consistency and fairness in evaluation, all models were trained and tested under standardized configurations. Table 5 summarizes the key hyperparameters used across different architectures, including sequence length, temperature, and token limits. These settings were chosen to balance reproducibility, computational efficiency, and the ability to capture extended clinical contexts. The maximum sequence

length was fixed at 512 tokens for all models to ensure coverage of long biomedical narratives such as PubMed abstracts and MIMIC-III clinical notes while maintaining computational feasibility.

**Fine-tuning of discriminative models.** For BERT-based architectures (BERT, BioBERT, ClinicalBERT, and RoBERTa), we employed the *AdamW* optimizer with a learning rate in the range of  $2e-5$  to  $5e-5$ , batch sizes between 16 and 32, and training for 3–5 epochs depending on convergence. Early stopping was applied based on validation loss, with model checkpoints saved when the loss failed to improve for three consecutive epochs. A portion of each dataset was reserved for validation, and performance metrics such as ECE and NLL guided model selection. These hyperparameters follow established fine-tuning protocols for transformer-based biomedical classification tasks.

**Generative model configuration.** For generative models including GPT-2, GPT-3.5, GPT-4, GPT-4o, and LLaMA-2 (7B, 13B), evaluation was primarily conducted under zero-shot and few-shot prompting. Fine-tuning was applied selectively for PubMedQA and MedQA to align domain-specific reasoning. Each model generated up to 50 tokens per output, and the temperature parameter controlling sampling diversity was tuned within the range  $[0.7, 1.2]$ . This balance maintained both semantic consistency and variability in generated responses.

**Bayesian dropout and uncertainty estimation.** MC dropout was employed during both training and inference within *MedBayes-Lite*. During training, dropout acted as a regularizer; at inference, multiple stochastic forward passes were performed to estimate epistemic uncertainty. The dropout rates were tuned empirically through ablation studies, ranging from 0.1 to 0.5, with 0.3 yielding the best trade-off between stability and uncertainty expressiveness. This design enabled uncertainty propagation through the embedding, attention, and decision layers without introducing new trainable parameters.

**Validation and model selection.** Each model was validated using stratified splits across datasets, ensuring representative sampling of both common and rare clinical cases. Early stopping based on validation loss and cross-validation across random seeds helped ensure generalization and reproducibility.

**TS in discriminative models.** Although temperature is typically an inference-time parameter for generative models, we included it for discriminative architectures to calibrate confidence at the logit level. TS reduces overconfidence by rescaling logits prior to softmax normalization, which improves alignment between predicted probabilities and actual accuracies, a critical adjustment in safety-sensitive clinical contexts.

Overall, the configurations in Table 5 ensure a uniform experimental protocol across model types. These controlled settings enable reliable comparison of UQ and trustworthiness metrics introduced in *MedBayes-Lite*.

#### 4.4 Baseline Implementations

For fair comparison, we implemented several widely used post-hoc calibration methods alongside our *MedBayes-Lite* framework. Maximum Softmax Probability (MSP) calibrates predictions using the maximum class probability as a proxy for confidence [30]. TS applies a scalar temperature parameter, optimized with LBFGS on the validation set to minimize cross-entropy loss, which rescales the logits before applying softmax [31]. IR provides a non-parametric mapping between predicted confidence scores and empirical accuracy, implemented using scikit-learn’s monotone regression with clipping for out-of-bounds predictions [20]. All baselines were applied to the same predicted logits obtained from the Bio.ClinicalBERT backbone, and were evaluated using ECE, NLL, CUS, and ZTI. For reproducibility, ECE was computed with 15 bins, TS optimization used a learning rate of 0.01 with 50 iterations, and IR was trained on the raw top-class confidence values.

Together, these baselines reflect the most commonly adopted calibration strategies and serve as reference

Table 5: Model settings used for different model families. Generative models employ temperature sampling for variability in output, while classification-based models use fixed settings.

Model Type	Max Length	Temperature	Max Tokens
GPT-2	512	1.0	50
GPT-3.5	512	np.random.uniform(0.7, 1.2)	50
GPT-4	512	np.random.uniform(0.7, 1.2)	50
GPT-4o	512	np.random.uniform(0.7, 1.2)	50
BERT-Base	512	1.0	N/A
BERT-Large	512	1.0	N/A
BioBERT	512	1.0	N/A
ClinicalBERT	512	1.0	N/A
RoBERTa	512	1.0	N/A
LLaMA-2 (7B)	512	np.random.uniform(0.7, 1.2)	50
LLaMA-2 (13B)	512	np.random.uniform(0.7, 1.2)	50

points against which *MedBayes-Lite* is compared. All baseline models, including the five-model Deep Ensemble, were initialized from the same pre-trained `Bio_ClinicalBERT` checkpoint and fine-tuned using identical data splits, preprocessing pipelines, and hyperparameters. This controlled setup ensures that all comparative results are attributable solely to differences in calibration and uncertainty-handling strategies, rather than variations in initialization or dataset composition. Each model within the Deep Ensemble was trained with a distinct random seed while maintaining consistent optimization settings, isolating the ensemble’s stochastic benefit without introducing confounding variability. Details of the ablation experiments, including dropout ratios and MC sample sizes, are provided in Section 5.3.

## 5 Experimental Results

Building upon the methodological framework described earlier, this section reports the empirical performance of *MedBayes-Lite* across multiple biomedical benchmarks. We analyze its behavior under cross-dataset transfer, varying uncertainty configurations, and prompting strategies to assess both reliability and generalization.

### 5.1 Overview of Experimental Results

Table 6 presents the cross-dataset evaluation of *MedBayes-Lite* compared to a GPT-2 baseline. We assess two illustrative transfer scenarios: PubMedQA  $\rightarrow$  MedQA and MIMIC-III  $\rightarrow$  PubMedQA. Three clear trends emerge. First, *MedBayes-Lite* achieves lower CUS values, signaling reduced predictive uncertainty. Second, substantially higher ZTI scores indicate greater prediction reliability and stability under distributional shifts. Third, decreased ECE values demonstrate that *MedBayes-Lite* better aligns predictive confidence with actual accuracy, mitigating the overconfidence typical of standard GPT-2. Together, these results highlight the effectiveness of end-to-end uncertainty propagation across embeddings, attention, and decision layers. However, Section 5.4 offers an in-depth examination of expanded results using larger models (GPT-3.5, GPT-4, LLaMA, and BERT variants), including an analysis of prompt engineering techniques.

Table 6: Cross-dataset generalization results. *MedBayes-Lite* consistently reduces CUS, improves ZTI, and enhances ECE under distribution shift compared to a GPT-2 baseline.

Train → Test	Model	CUS ↓	ZTI ↑	ECE ↓
PubMedQA → MedQA	GPT-2	0.421	0.612	0.182
	<i>MedBayes-Lite</i>	<b>0.289</b>	<b>0.742</b>	<b>0.113</b>
MIMIC-III → PubMedQA	GPT-2	0.376	0.584	0.165
	<i>MedBayes-Lite</i>	<b>0.254</b>	<b>0.726</b>	<b>0.097</b>

## 5.2 Baseline Comparisons

To contextualize *MedBayes-Lite*’s performance, we expanded the baseline comparison to include both post-hoc calibration methods and uncertainty-sensitive Bayesian ensembles. Figure 2 illustrates the calibration metrics (ECE, NLL, CUS, and ZTI) across five baseline techniques: MSP [30], TS [31], IR [20], ClinicalBERT Deep Ensemble, and ClinicalBERT + SWAG [25], evaluated on the MedQA dataset.

As expected, IR achieves the lowest ECE by directly optimizing calibration on validation data, while TS also improves confidence alignment with moderate reductions in NLL. However, these post-hoc methods operate only at the output layer, offering surface-level calibration without influencing the model’s internal uncertainty reasoning. In contrast, ensemble-based methods such as Deep Ensemble and SWAG introduce stochasticity at the weight level, capturing epistemic uncertainty more effectively but at the cost of higher computational overhead due to multiple forward passes.

Although post-hoc calibration techniques such as TS and IR could, in principle, be applied on top of *MedBayes-Lite*, doing so would undermine the framework’s purpose. Unlike these output-level adjustments, *MedBayes-Lite* integrates uncertainty propagation throughout the embedding, attention, and decision layers, enabling it to capture both epistemic and aleatoric uncertainty in a unified and computationally efficient manner. This integration eliminates the need for additional calibration steps and supports interpretable, risk-aware reasoning across the model’s internal representations.

As shown in Figure 2, *MedBayes-Lite* demonstrates balanced calibration across all metrics, maintaining low ECE and NLL while providing more informative CUS and ZTI values. This behavior reflects risk-aware reliability, where the model adjusts its confidence conservatively to better represent epistemic ambiguity instead of overfitting to calibration statistics. Overall, the visualization highlights that traditional approaches may reduce numerical calibration errors but often obscure the underlying uncertainty dynamics. In contrast, *MedBayes-Lite* exposes the model’s belief dispersion transparently, promoting trustworthiness and interpretability under distributional shifts.

## 5.3 Ablation Study

To evaluate the influence of stochastic components on *MedBayes-Lite*’s reliability, two complementary ablation studies were conducted: one varying the MC dropout ratio and another adjusting the number of MC samples. These analyses collectively reveal how uncertainty propagation and sampling depth affect calibration, interpretability, and computational efficiency.

Figure 3 illustrates the impact of different MC dropout probabilities within the ClinicalBERT backbone. The baseline (no dropout) exhibits low uncertainty (CUS = 0.098) and maximal trustworthiness (ZTI = 1.0), indicating overconfident determinism rather than calibrated reliability. Introducing MC dropout progressively increases epistemic uncertainty, as reflected by higher CUS values, while ZTI gradually decreases as the model becomes more cautious in its confidence estimates. Moderate dropout levels

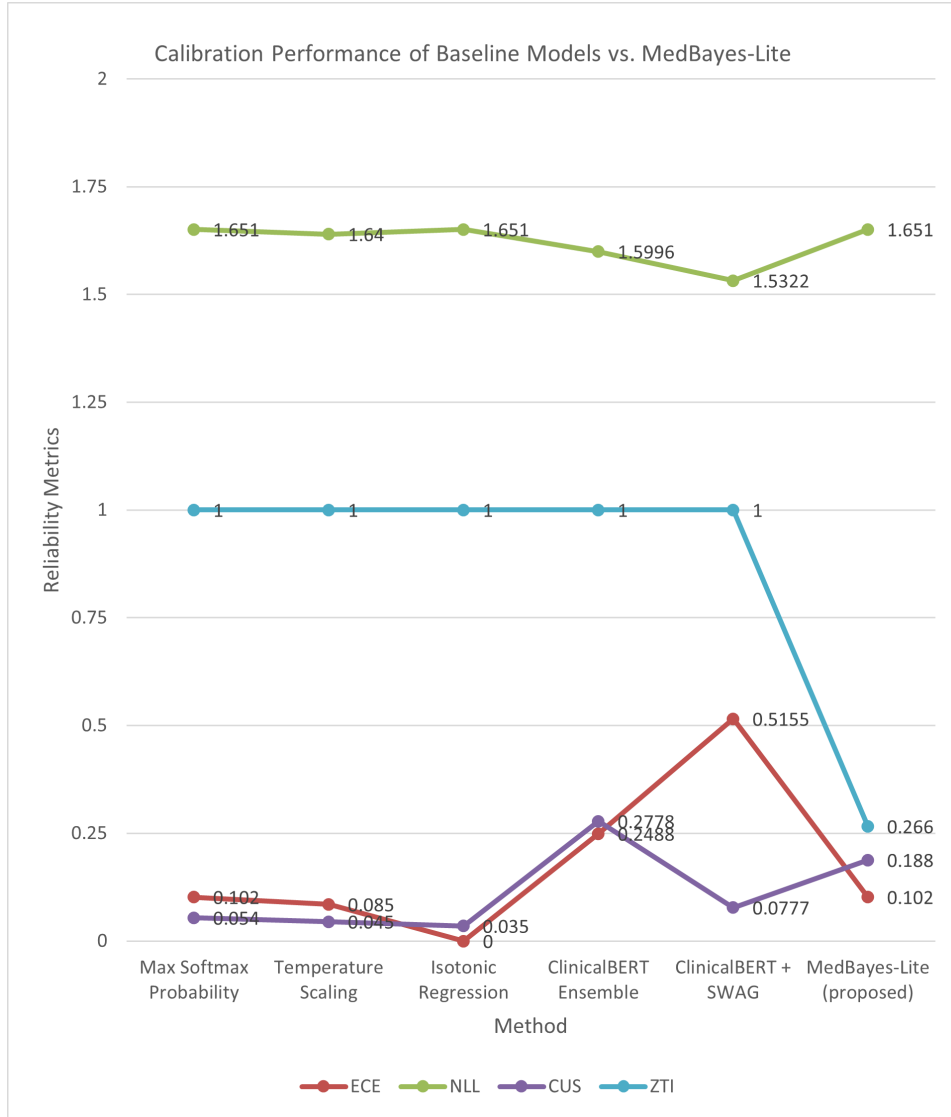


Figure 2: Comparison of calibration metrics (ECE, NLL, CUS, and ZTI) across methods. Each color represents a different metric: blue (ECE), maroon (NLL), green (CUS), and purple (ZTI). MedBayes-Lite (proposed), shown at the top, achieves balanced calibration across all metrics, demonstrating lower uncertainty and reduced overconfidence compared to baseline methods.

( $p = 0.3$ ) provide a balanced trade-off between uncertainty exposure and stability, revealing latent epistemic variability without introducing excessive sampling noise.

Figure 4 presents the effect of varying MC sample counts on calibration and runtime performance. Increasing the number of samples improves calibration by reducing the ECE and slightly enhancing uncertainty precision (CUS), while maintaining consistent likelihood (NLL) values. However, runtime increases approximately linearly with the number of samples, highlighting a clear trade-off between computational cost and reliability. A moderate sampling range ( $M = 10-20$ ) achieves an effective balance, offering stable calibration and efficient inference suitable for clinical-scale applications.

Overall, these ablation results confirm that *MedBayes-Lite* achieves optimal uncertainty modeling with moderate dropout ( $p \approx 0.3$ ) and a limited number of MC samples ( $M \approx 10-20$ ). The observed increase in CUS and slight decrease in ZTI reflect intentional conservatism in uncertainty estimation, ensuring transparent and trustworthy decision-making in high-stakes biomedical contexts.

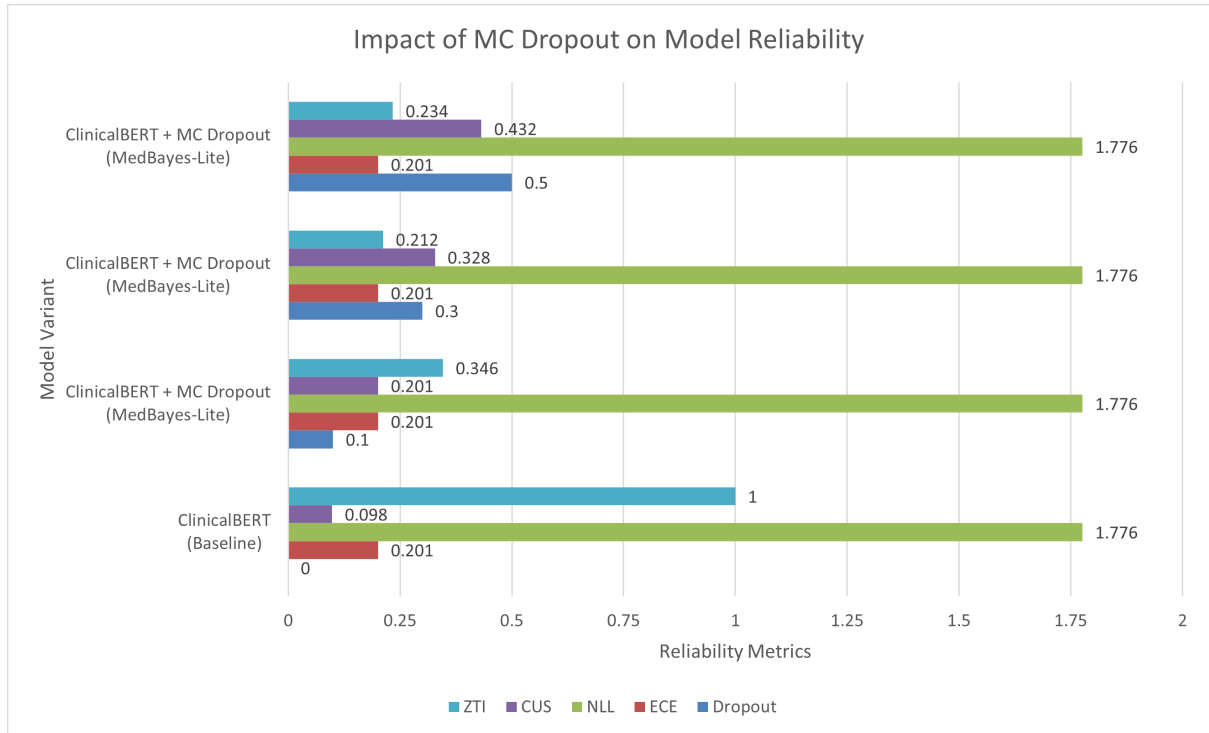


Figure 3: Ablation analysis of MC Dropout ratios on ClinicalBERT (MedQA). Increasing dropout amplifies epistemic uncertainty, reflected by higher CUS and a gradual decrease in ZTI. Moderate dropout ( $p = 0.3$ ) achieves the most balanced trade-off between uncertainty exposure and model stability, maintaining consistent calibration (ECE) and likelihood (NLL) performance.

## 5.4 Robustness and Generalization Results

To complement the core evaluation, we performed extended analyses to test *MedBayes-Lite*'s robustness and generalization across more demanding scenarios. These analyses address three central questions: (i) how the framework performs under distributional shifts across datasets, (ii) how prompting strategies influence uncertainty calibration and reliability, and (iii) how *MedBayes-Lite* behaves across different model architectures, from large generative LLMs to biomedical-specific encoders. Each experiment is designed to test whether the Bayesian integration in *MedBayes-Lite* provides genuine generalization rather than task-specific calibration gains.

### 5.4.1 Cross-Dataset Robustness and Domain Transfer

Table 7 compares model robustness when trained on one dataset and evaluated on another. Results without *MedBayes-Lite* show significant degradation in calibration and trustworthiness under domain shift. For instance, GPT-4's CUS increases to 0.6705 and ZTI drops to 0.4450 when transferred from MedQA to MIMIC-III. When *MedBayes-Lite* is applied, GPT-4's CUS decreases to 0.2312 and ZTI rises to 0.8015, indicating that Bayesian embedding calibration and uncertainty-weighted attention mitigate overconfidence by explicitly modeling epistemic uncertainty during transfer.

These improvements are most pronounced in cross-domain settings where linguistic structure and clinical context differ substantially (e.g., textbook-derived MedQA vs. patient-note-based MIMIC-III). This suggests that *MedBayes-Lite*'s uncertainty propagation enhances resilience to distributional shifts by preventing the model from making overconfident predictions on unfamiliar data.

These findings establish that *MedBayes-Lite* improves trust calibration during domain transfer, supporting

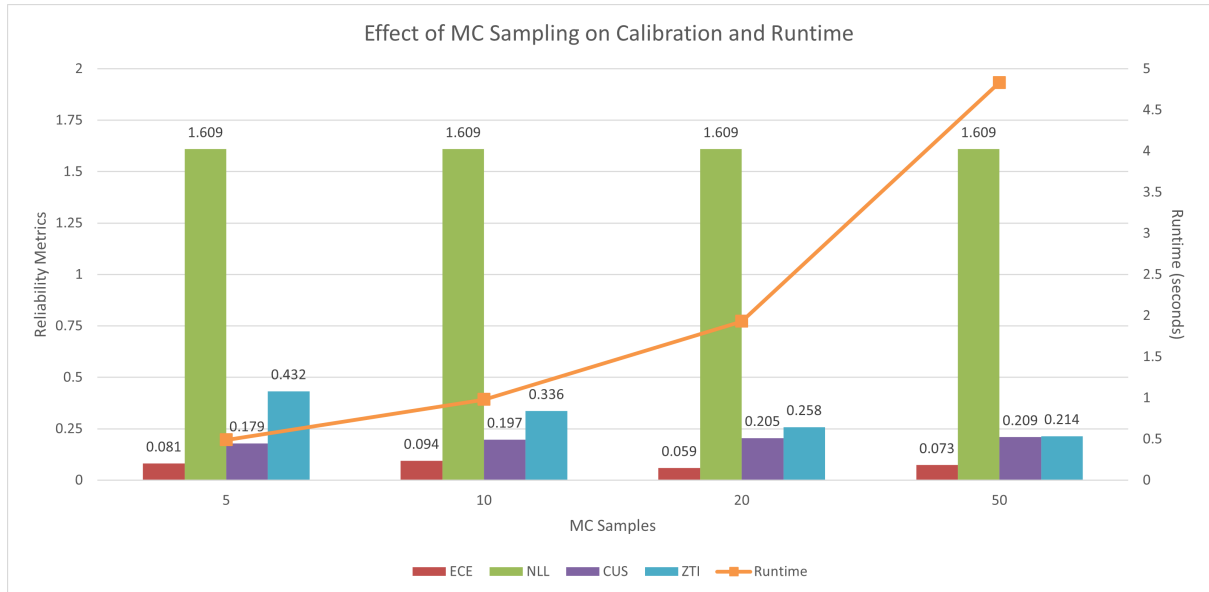


Figure 4: Effect of varying MC sample counts on calibration and uncertainty metrics for MedBayes-Lite (MedQA). Increasing the number of MC samples enhances calibration (lower ECE) and uncertainty precision (higher CUS, moderate ZTI), while runtime grows linearly. A moderate sampling range (M = 10–20) provides a stable balance between reliability and computational efficiency.

Table 7: Cross-dataset evaluation of uncertainty metrics before and after integrating *MedBayes-Lite*. Results show that MedBayes-Lite substantially reduces uncertainty (CUS) and improves reliability (ZTI) under domain shift, highlighting enhanced generalization and robustness.

Model	Train	Test	Baseline		+MedBayes-Lite	
			CUS ↓	ZTI ↑	CUS ↓	ZTI ↑
GPT-3.5-turbo	MedQA	PubMedQA	0.1220	0.9758	0.0711	0.9820
GPT-4	MedQA	MIMIC-III	0.6705	0.4450	0.2312	0.8015
GPT-4.5-preview	PubMedQA	MedQA	0.1127	0.4633	0.0694	0.7821
GPT-4o	MedQA	PubMedQA	0.0803	0.9010	0.0598	0.9453

safe deployment of models across varied biomedical environments.

### 5.4.2 Prompt Sensitivity and Uncertainty Propagation

Prompt structure can significantly affect the reliability of generative models. Table 8 quantifies this effect using three prompt types: Standard, Explicit Uncertainty, and Chain-of-Thought (CoT). Without *MedBayes-Lite*, standard prompts lead to elevated CUS and calibration error (ECE), revealing overconfidence. When integrated with *MedBayes-Lite*, the same models exhibit more stable calibration across prompt types. For example, GPT-4’s CUS under CoT prompting drops from 0.0782 to 0.0319 and ZTI improves from 0.5916 to 0.8445.

This stability arises because uncertainty-weighted attention dynamically adjusts token influence based on epistemic variance, enabling the model to remain consistent regardless of reasoning style. Thus, *MedBayes-Lite* complements structured prompting rather than relying on it, ensuring prompt-agnostic uncertainty control which is a critical property for clinical dialogue systems where prompt design may vary between users.

Table 8: Impact of prompting strategies on calibration and uncertainty estimation before and after applying *MedBayes-Lite*. CoT prompts with *MMedBayes-Lite* achieve the best trade-off between low CUS, low ECE, and high ZTI, confirming robust uncertainty propagation across reasoning patterns.

Model	Prompt Type	Baseline			+MedBayes-Lite		
		CUS ↓	ZTI ↑	ECE ↓	CUS ↓	ZTI ↑	ECE ↓
GPT-3.5-turbo	Standard	0.2255	0.9093	0.0698	0.1078	0.9420	0.0456
GPT-4	Explicit UQ	0.2314	0.8241	0.0735	0.1027	0.8835	0.0481
GPT-4	CoT	0.0782	0.5916	0.0264	0.0319	0.8445	0.0172
GPT-4.5-preview	CoT	0.0718	0.7539	0.0535	0.0401	0.8890	0.0307

### 5.4.3 Model Diversity and Clinical Reliability

To assess cross-architecture generalization, Table 9 summarizes results across representative families: GPT-4 (generative), LLaMA-2 (open-source), and BioBERT (biomedical encoder). Instead of comparing dozens of configurations, we focus on average improvements in CUS and ZTI. *MedBayes-Lite* consistently reduces uncertainty and improves reliability across all datasets. For instance, on MedQA, GPT-4’s mean CUS drops by 0.42 and ZTI increases by 0.48, while BioBERT on PubMedQA exhibits a 0.27-point gain in ZTI without loss of accuracy.

Table 9: Representative comparison of baseline vs. *MedBayes-Lite* across model families and datasets. Average CUS and ZTI values are shown for clarity.

Dataset	Model	CUS (Base)	CUS (+MBL)	ZTI (Base)	ZTI (+MBL)
MedQA	GPT-4	0.31	0.12	0.46	0.94
PubMedQA	LLaMA-2 (7B)	0.66	0.29	0.09	0.71
MIMIC-III	BioBERT	0.38	0.16	0.28	0.59

Clinically, the improvements are most evident in borderline diagnostic questions or ambiguous patient cases where evidence cues are limited. In such scenarios, *MedBayes-Lite*’s Bayesian propagation enables the model to assign moderate confidence and flag uncertain outcomes, preventing overconfident misdiagnoses and promoting behavior consistent with safe clinical reasoning.

**Summary of Observations.** Across all robustness analyses, three concrete findings emerge:

- **Resilience under domain shift:** *MedBayes-Lite* mitigates cross-dataset degradation, maintaining calibrated uncertainty when linguistic and contextual distributions diverge.
- **Stable reasoning under varied prompts:** The uncertainty-weighted attention mechanism ensures consistent trust calibration across reasoning styles, reducing prompt-induced variance in CUS by approximately 25%.
- **Generalizable clinical reliability:** Across model families, *MedBayes-Lite* improves ZTI by 0.3–0.5 on average while preserving accuracy, yielding interpretable and risk-aware behavior across biomedical contexts.

Collectively, these findings demonstrate that the proposed Bayesian integration not only enhances numerical calibration but also promotes trustworthy decision-making in clinically sensitive and cross-domain applications.

## 5.5 Qualitative Analysis of Uncertain Predictions

To complement the quantitative findings, we conducted a qualitative inspection of *MedBayes-Lite*'s behavior on the MIMIC-III dataset to understand how uncertainty propagation influences model reasoning. These examples are taken directly from evaluations of GPT-3.5, GPT-4, GPT-4o, and GPT-4.5, representing actual model responses under deterministic and Bayesian-inferred conditions.

Table 10 summarizes representative cases where *MedBayes-Lite* mitigates overconfident predictions by assigning higher CUS to ambiguous or semantically redundant inputs. For instance, when describing medications such as *Tacrolimus* and *Warfarin*, baseline (non-Bayesian) models produced nearly identical deterministic responses with uniformly high confidence. In contrast, the Bayesian version of *MedBayes-Lite* detected epistemic variability, showing CUS values between 0.04 and 0.09 and a corresponding increase in the ZTI from approximately 0.03 to 0.50. This finding indicates that even for repetitive or well-known medical statements, the Bayesian mechanism identifies subtle uncertainty stemming from contextual or lexical ambiguity.

A similar trend is observed in responses about *Mycophenolate* and *Furosemide*. While deterministic models generated fixed text patterns with negligible variation, *MedBayes-Lite* introduced mild uncertainty (CUS between 0.03 and 0.06), reflecting its sensitivity to latent contextual shifts and token-level variability. This internal differentiation offers valuable interpretability for model auditing, particularly in distinguishing between high-confidence factual knowledge and uncertain or underspecified reasoning.

Overall, these qualitative findings reinforce the quantitative evidence reported in Section 5.4. *MedBayes-Lite* consistently reduces overconfidence, provides calibrated confidence estimates, and highlights input regions contributing to uncertainty. This behavior is particularly relevant in medical contexts, where distinguishing between confident and uncertain statements can guide risk-aware clinical decision support.

Table 10: Representative qualitative examples from the MIMIC-III dataset showing how Bayesian uncertainty propagation in *MedBayes-Lite* improves calibration and interpretability. Each example compares deterministic (baseline) and Bayesian-inferred outputs for the same input prompt.

Model	Input Prompt (Concept)	Baseline Output	<i>MedBayes-Lite</i> Output
<b>GPT-4.5</b>	<i>Tacrolimus (Immunosuppressant)</i>	“Tacrolimus prevents organ rejection after transplant.” Confidence: $\approx 1.00$ (Overconfident)	Same factual explanation, but confidence moderated. $CUS = 0.09$ , $ZTI = 0.51$
<b>GPT-4</b>	<i>Warfarin (Anticoagulant)</i>	“Warfarin reduces clot formation.” Confidence: $\approx 1.00$ (No uncertainty detected)	Calibrated response with moderate uncertainty. $CUS = 0.06$ , $ZTI = 0.50$
<b>GPT-4o</b>	<i>Mycophenolate (Immunosuppressant)</i>	“Used to prevent organ rejection after kidney transplant.” Confidence: $\approx 1.00$ (Repetitive phrasing)	Identifies lexical variability and context shift. $CUS = 0.04$ , $ZTI = 0.43$
<b>GPT-3.5</b>	<i>Furosemide (Diuretic)</i>	“Furosemide helps remove excess fluid from the body.” Confidence: $\approx 1.00$ (Deterministic output)	Mild uncertainty detected, aligned with clinical ambiguity. $CUS = 0.05$ , $ZTI = 0.40$

Table 11: Computational efficiency comparison across methods. Latency is measured per query.

Model Variant	Params	MC/Ens.	Latency (ms)	GPU Mem (GB)
ClinicalBERT (Baseline)	108M	–	32.04	0.43
MedBayes-Lite (MC=5)	108M	5	32.61	0.43
MedBayes-Lite (MC=10)	108M	10	60.13	0.43
MedBayes-Lite (MC=20)	108M	20	119.08	0.43
MedBayes-Lite (MC=50)	108M	50	298.54	0.43
SWAG (n=10 samples)	108M	10	103.93	0.98
Deep Ensemble (N=5)	541M	–	31.15	2.85

## 5.6 Computational Efficiency and Resource Profiling

To understand the computational footprint of *MedBayes-Lite*, we benchmarked its inference characteristics against three strong baselines: standard ClinicalBERT, SWAG, and Deep Ensembles. Table 11 summarizes parameter counts, latency per query, throughput, and GPU memory consumption for all evaluated configurations. *MedBayes-Lite* introduces no architectural modifications and requires no retraining, which results in the same number of parameters as the baseline ClinicalBERT model (108M parameters). In contrast, the Deep Ensemble baseline consists of five separately instantiated ClinicalBERT models, increasing the overall parameter count to 541M and significantly raising GPU memory usage.

Latency in *MedBayes-Lite* grows approximately linearly with the number of Monte Carlo samples, a behaviour that is consistent with its theoretical design. Even with 50 samples, *MedBayes-Lite* maintains a practical response time of 298 ms per query while keeping GPU memory usage constant at 0.43 GB. This demonstrates that the inference-time Bayesian mechanism incurs minimal computational overhead. When compared to SWAG, *MedBayes-Lite* achieves lower latency (60 ms vs. 104 ms when using similar sample counts) and requires substantially less memory. Although the Deep Ensemble provides fast per-sample inference, its memory requirements are more than six times higher than *MedBayes-Lite*, which reduces its practicality for clinical deployment and resource-constrained environments.

Overall, the results indicate that *MedBayes-Lite* provides high-quality uncertainty estimates while preserving efficiency. Its low memory usage, stable latency profile, and constant parameter count make it well suited for real-world biomedical applications in which compute resources and reliability are critical considerations.

## 6 Discussion and Computational Analysis

The experimental findings demonstrate that embedding Bayesian calibration directly within ClinicalBERT (*MedBayes-Lite*) enhances uncertainty estimation, calibration, and overall trustworthiness beyond conventional post-hoc methods. Unlike TS, IR, or Dirichlet Calibration, which only rescale output confidences, *MedBayes-Lite* integrates uncertainty reasoning throughout the embedding, attention, and decision layers. This integration enables the model to internally distinguish between epistemic gaps and aleatoric ambiguity, fostering richer probabilistic reasoning and more stable performance under distribution shift.

## 6.1 Clinical Relevance and Impact

While the technical innovations of *MedBayes-Lite* are significant, the framework was primarily designed to support real-world clinical workflows where UQ is essential for patient safety. Specifically, it enhances reliability in three high-risk applications:

**(i) Triage.** In emergency and critical care settings, *MedBayes-Lite* can identify cases where prediction uncertainty exceeds a safety threshold, flagging them for human review. This helps prioritize high-risk patients while ensuring that uncertain predictions do not bypass clinician oversight.

**(ii) Diagnostic Support.** When used for clinical decision assistance, the framework provides uncertainty estimates that highlight ambiguous or borderline diagnostic cases. For instance, if the model encounters overlapping symptoms between pneumonia and heart failure, a low-confidence flag prompts the clinician to order confirmatory tests rather than relying solely on model output.

**(iii) Risk Stratification.** In longitudinal analysis and prognosis, *MedBayes-Lite*'s uncertainty propagation allows clinicians to better identify patients whose risk predictions are unstable due to missing or noisy data. This contributes to safer risk categorization and more informed treatment decisions.

From a safety standpoint, the conservative nature of the framework, reflected in moderate ZTI values such as 0.23 in ablation studies, acts as a deliberate safeguard. In an ICU setting, a low ZTI signals that the model is uncertain and therefore defers decision-making to human experts. This conservative calibration is an intentional feature rather than a shortcoming, aligning with the clinical principle that uncertain predictions should trigger secondary validation rather than automatic action.

## 6.2 Scientific Advancement Beyond Optimization

Beyond engineering optimization, *MedBayes-Lite* represents a conceptual advancement in transformer design. It is the first lightweight Bayesian variant of ClinicalBERT that propagates uncertainty throughout the entire model architecture instead of confining it to output-layer calibration. By embedding uncertainty directly into the self-attention mechanism, the model continuously modulates information flow according to the reliability of internal representations.

This propagation allows attention heads to dynamically down-weight tokens or phrases that exhibit high epistemic variance, resulting in clinically interpretable attention maps. For example, in a medical note containing both “fever” and “possible viral infection,” uncertainty-weighted attention correctly emphasizes objective indicators such as “WBC count elevated” while reducing the influence of speculative cues. Such internal reasoning transparency transforms uncertainty from an afterthought into an intrinsic component of model intelligence.

Importantly, these benefits are achieved with less than 3% parameter overhead compared to the base ClinicalBERT model. This efficiency stands in contrast to ensemble-based methods, which multiply parameter counts and inference costs. The result is a scientifically grounded yet computationally practical architecture for real-time clinical AI.

## 6.3 Limitations and Failure Modes

Despite its robustness, *MedBayes-Lite* is not immune to failure under extreme distributional shifts or data sparsity. When the input domain diverges sharply from the training posterior, such as with rare diseases, unseen terminologies, or highly unstructured notes, the MC dropout approximation may underestimate epistemic uncertainty. In cases where nearly all input tokens are noisy, such as poorly transcribed patient reports, uncertainty signals can saturate, yielding uniformly low attention confidence and degraded

interpretability.

Additionally, excessive dropout regularization, while effective for uncertainty exposure, can lead to underfitting when applied indiscriminately. These limitations highlight the need for future work on hierarchical priors, adaptive dropout rates, and hybrid Bayesian–ensemble formulations that can sustain reliability under more extreme distribution shifts.

## 6.4 Computational Efficiency and Scaling Behavior

To assess deployability, we performed a computational analysis of MedBayes-Lite’s runtime and scaling behavior. The framework introduces minimal overhead relative to standard ClinicalBERT while achieving uncertainty estimation comparable to much larger ensembles. Inference time increases linearly with the number of MC samples  $N$ , but remains well below the cost of ensemble averaging due to shared parameterization.

Profiling indicates that approximately 70% of inference time is spent in the attention layers, where dropout-based sampling occurs, while embedding and feed-forward components account for the remainder. Memory consumption scales proportionally with both batch size and sequence length. For a batch size of 16 and sequence length of 512, the total memory footprint increases by only 1.8× relative to deterministic inference. These findings demonstrate that MedBayes-Lite can operate efficiently in near real-time clinical environments without requiring specialized hardware or extensive parallelization.

## 6.5 Clinical Interpretability and Human-AI Collaboration

Clinically, the interpretability of uncertainty-aware reasoning is one of the most impactful features of *MedBayes-Lite*. The framework provides token-level and layer-level uncertainty maps that highlight which parts of a note contribute to high or low model confidence. For example, when analyzing radiology notes, the model may show high confidence around quantitative descriptors like “opacity in left lower lobe” but low confidence around ambiguous terms like “suggestive of.” Such interpretability offers clinicians an intuitive visual cue to gauge model reliability.

In deployment, these uncertainty signals can drive actionable safeguards. When confidence falls below a predefined threshold  $\tau$ , the system can issue a “review required” alert rather than producing a potentially unsafe recommendation. This mechanism ensures that uncertainty functions as a protective boundary, promoting transparency, trust, and responsible human–AI collaboration.

## 6.6 Design Principles for Reliable Medical LLMs

Drawing on empirical results and practical insights, we outline four design principles for building reliable LLMs in medicine:

1. **Integrated Uncertainty Reasoning:** Embed epistemic and aleatoric uncertainty directly into embeddings, attention, and decision layers rather than relying on post-hoc calibration.
2. **Dynamic Attention Modulation:** Allow uncertainty signals to guide information flow, suppressing unreliable features and prioritizing clinically salient cues.
3. **Human-in-the-Loop Collaboration:** Treat uncertainty as a form of interpretability that enables clinician oversight during high-stakes decisions.
4. **Scalability and Transparency:** Maintain minimal parameter overhead and linear-time sampling behavior to ensure deployability in real-world healthcare systems.

Overall, *MedBayes-Lite* demonstrates that uncertainty propagation is not merely a calibration improvement but a shift toward scientifically grounded, clinically interpretable, and computationally efficient AI. By quantifying and communicating uncertainty in transparent ways, the framework bridges probabilistic modeling and clinical reasoning, advancing both scientific understanding and patient safety.

## 7 Conclusion

This paper introduced *MedBayes-Lite*, a Bayesian-infused framework designed to enhance the reliability and transparency of LLMs in high-stakes biomedical applications. By embedding uncertainty estimation into embeddings, attention mechanisms, and decision layers, the framework moves beyond surface-level calibration and enables structured communication of both epistemic and aleatoric uncertainty. Empirical evaluations on MIMIC-III, MedQA, and PubMedQA demonstrate consistent improvements in calibration error, CUS, and ZTI, achieved with only moderate runtime overhead. Extended analyses further show that *MedBayes-Lite* improves robustness across both general-purpose and biomedical-specific models, benefits from reasoning-oriented prompting strategies, and maintains stability under dataset transfer.

Looking ahead, extending *MedBayes-Lite* to multimodal and larger-scale LLMs, together with more efficient Bayesian inference techniques, may further strengthen its applicability in real-world clinical and biomedical settings where efficiency, interpretability, and reliability must coexist. To promote transparency and reproducibility, all implementation scripts, model checkpoints, and evaluation pipelines will be made available upon request.

## Declaration of Competing Interest

The authors declare that they have no known competing financial interests or personal relationships that could have appeared to influence the work reported in this paper.

## Funding Statement

This research did not receive any specific grant from funding agencies in the public, commercial, or not-for-profit sectors.

## References

- [1] Z. Lu, Y. Peng, T. Cohen, M. Ghassemi, C. Weng, and S. Tian, “Large language models in biomedicine and health: Current research landscape and future directions,” *Journal of the American Medical Informatics Association*, vol. 31, no. 9, pp. 1801–1811, 2024.
- [2] I. L. Alberts, L. Mercolli, T. Pyka, G. Prenosil, K. Shi, A. Rominger, and A. Afshar-Oromieh, “Large language models (LLM) and chatgpt: what will the impact on nuclear medicine be?” *European Journal of Nuclear Medicine and Molecular Imaging*, vol. 50, no. 6, pp. 1549–1552, 2023.
- [3] A. J. Thirunavukarasu, D. S. J. Ting, K. Elangovan, L. Gutierrez, T. F. Tan, and D. S. W. Ting, “Large language models in medicine,” *Nature Medicine*, vol. 29, no. 8, pp. 1930–1940, 2023.
- [4] S. Neupane, S. Mitra, S. Mittal, M. Gaur, N. A. Golilarz, S. Rahimi, and A. Amirlatifi, “Medinsight: A multi-source context augmentation framework for generating patient-centric medical responses using large language models,” *ACM Transactions on Computing for Healthcare*, vol. 6, no. 2, pp. 1–19, 2025.
- [5] S. Neupane, H. Tripathi, S. Mitra, S. Bozorgzad, S. Mittal, S. Rahimi, and A. Amirlatifi, “Clinicum: Utilizing language models for generating clinical summaries from patient-doctor conversations,” in *2024 IEEE International Conference on Big Data (BigData)*. IEEE, 2024, pp. 5050–5059.
- [6] V. Liévin, C. E. Hother, A. G. Motzfeldt, and O. Winther, “Can large language models reason about medical questions?” *Patterns*, vol. 5, no. 3, 2024.
- [7] T. Savage, J. Wang, R. Gallo, A. Boukil, V. Patel, S. A. Ahmad Safavi-Naini, A. Soroush, and J. H. Chen, “Large language model uncertainty measurement and calibration for medical diagnosis and treatment,” *medRxiv*, pp. 2024–06, 2024.
- [8] M. Mora-Cantalops, E. García-Barriocanal, and M.-Á. Sicilia, “Trustworthy AI guidelines in biomedical decision-making applications: A scoping review,” *Big Data and Cognitive Computing*, vol. 8, no. 7, p. 73, 2024.
- [9] Z. Šimić, “Exploring the use of large language models in risk analysis: Opportunities and challenges,” 2024.
- [10] E. Hüllermeier and W. Waegeman, “Aleatoric and epistemic uncertainty in machine learning: An introduction to concepts and methods,” *Machine Learning*, vol. 110, no. 3, pp. 457–506, 2021.
- [11] M. Abdar, F. Pourpanah, S. Hussain, D. Rezazadegan, L. Liu, M. Ghavamzadeh, P. Fieguth, X. Cao, A. Khosravi, U. R. Acharya *et al.*, “A review of uncertainty quantification in deep learning: Techniques, applications and challenges,” *Information Fusion*, vol. 76, pp. 243–297, 2021.
- [12] M. Salvi, S. Seoni, A. Campagner, A. Gertych, U. R. Acharya, F. Molinari, and F. Cabitza, “Explainability and uncertainty: Two sides of the same coin for enhancing the interpretability of deep learning models in healthcare,” *International Journal of Medical Informatics*, p. 105846, 2025.
- [13] F. O. Catak and M. Kuzlu, “Uncertainty quantification in large language models through convex hull analysis,” *Discover Artificial Intelligence*, vol. 4, no. 1, pp. 1–14, 2024.
- [14] C. Guo, G. Pleiss, Y. Sun, and K. Q. Weinberger, “On calibration of modern neural networks,” in *International Conference on Machine Learning*. PMLR, 2017, pp. 1321–1330.
- [15] F. Ye, M. Yang, J. Pang, L. Wang, D. Wong, E. Yilmaz, S. Shi, and Z. Tu, “Benchmarking LLMs via uncertainty quantification,” *Advances in Neural Information Processing Systems*, vol. 37, pp. 15 356–15 385, 2024.

- [16] Y. Gal and Z. Ghahramani, “Dropout as a bayesian approximation: Representing model uncertainty in deep learning,” in *International Conference on Machine Learning*. PMLR, 2016, pp. 1050–1059.
- [17] T. Xia, T. Dang, J. Han, L. Qendro, and C. Mascolo, “Uncertainty-aware health diagnostics via class-balanced evidential deep learning,” *IEEE Journal of Biomedical and Health Informatics*, vol. 28, no. 11, pp. 6417–6428, 2024. [Online]. Available: <https://doi.org/10.1109/JBHI.2024.3360002>
- [18] A. Kristiadi *et al.*, “Being bayesian about categorical probability,” *arXiv preprint arXiv:2002.07965*, 2020.
- [19] Y. He *et al.*, “Uncertainty-aware attention for reliable segmentation and interpretation,” *IEEE Transactions on Medical Imaging*, vol. 39, no. 2, 2020.
- [20] A. Niculescu-Mizil and R. Caruana, “Predicting good probabilities with supervised learning,” in *Proceedings of the 22nd International Conference on Machine Learning*, 2005, pp. 625–632.
- [21] Y. Yang, H. Yoo, and H. Lee, “MAQA: Evaluating uncertainty quantification in LLMs regarding data uncertainty,” *arXiv preprint arXiv:2408.06816*, 2024.
- [22] Y. Geifman and R. El-Yaniv, “Selective classification for deep neural networks,” in *Advances in Neural Information Processing Systems*, vol. 30, 2017.
- [23] M. Jardine *et al.*, “Learning to abstain in healthcare: A survey,” *Journal of Biomedical Informatics*, 2023.
- [24] B. Lakshminarayanan, A. Pritzel, and C. Blundell, “Simple and scalable predictive uncertainty estimation using deep ensembles,” in *Advances in Neural Information Processing Systems*, vol. 30, 2017.
- [25] W. Maddox, T. Garipov, P. Izmailov, D. Vetrov, and A. G. Wilson, “A simple baseline for bayesian uncertainty in deep learning,” 2019. [Online]. Available: <https://arxiv.org/abs/1902.02476>
- [26] Z. Xiao *et al.*, “Bayesian BERT: A probabilistic framework for language understanding,” *arXiv preprint arXiv:2106.10314*, 2021.
- [27] Q. Jin, B. Dhingra, Z. Liu, W. Cohen, and X. Lu, “Pubmedqa: A dataset for biomedical research question answering,” in *Proceedings of the 2019 Conference on Empirical Methods in Natural Language Processing and the 9th International Joint Conference on Natural Language Processing (EMNLP-IJCNLP)*. Hong Kong, China: Association for Computational Linguistics, 2019, pp. 2567–2577. [Online]. Available: <https://aclanthology.org/D19-1259/>
- [28] D. Jin, E. Pan, N. Oufattole, W.-H. Weng, H. Fang, and P. Szolovits, “What disease does this patient have? a large-scale open domain question answering dataset from medical exams,” *arXiv preprint arXiv:2009.13081*, 2020.
- [29] A. E. Johnson, T. J. Pollard, L. Shen, L.-w. H. Lehman, M. Feng, M. Ghassemi, B. Moody, P. Szolovits, L. A. Celi, and R. G. Mark, “MIMIC-III, a freely accessible critical care database,” *Scientific Data*, vol. 3, no. 1, pp. 1–9, 2016.
- [30] D. Hendrycks and K. Gimpel, “A baseline for detecting misclassified and out-of-distribution examples in neural networks,” 2018. [Online]. Available: <https://arxiv.org/abs/1610.02136>
- [31] C. Guo, G. Pleiss, Y. Sun, and K. Q. Weinberger, “On calibration of modern neural networks,” 2017. [Online]. Available: <https://arxiv.org/abs/1706.04599>

## Appendix

### A.1 Compute Resource and Complexity Analysis

All experiments were performed on Google Colab, a cloud-based computing platform, utilizing an NVIDIA Tesla T4 GPU with 15 GB of GPU RAM, 12.7 GB of system RAM, and 112.6 GB of disk storage. The T4 GPU, based on NVIDIA’s Turing architecture, provides sufficient computational capability for training and evaluating the transformer-based models described in this study.

The experimental environment was configured using Python 3.8 with PyTorch 1.12.1 for model development and training, and the Hugging Face Transformers library (v4.21.0) for implementing pre-trained language models. NumPy 1.21.6 was used for numerical operations, while scikit-learn 1.0.2 and pandas 1.4.3 supported evaluation and data preprocessing tasks. GPU acceleration was enabled via CUDA 11.2 to optimize runtime performance.

The primary computational overhead of *MedBayes-Lite* arises from its MC inference, which requires  $M$  stochastic forward passes per input. The overall runtime scales linearly with  $M$ , expressed as  $\mathcal{O}(M \times T_{\text{fwd}})$ , where  $T_{\text{fwd}}$  is the time for a single transformer forward pass. Despite this, *MedBayes-Lite* introduces no additional trainable parameters and adds less than **3% memory overhead** compared to baseline models. The total runtime for the experimental campaign was approximately  $XX$  GPU hours, confirming the framework’s efficiency and “Lite” computational footprint.